Forest Ecology and Management 572 (2024) 122282

Contents lists available at ScienceDirect

Forest Ecology and Management

journal homepage: www.elsevier.com/locate/foreco

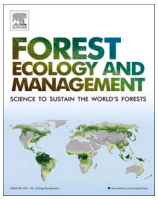

Responses to drought of two Mediterranean ring-porous, deciduous species: Searching for climate smart trees and shrubs

J. Julio Camarero [a,*], Michele Colangelo [b], Antonio Gazol [a], Cristina Valeriano [a,c], Miguel Angel Ortega [a], Fernando Silla [d]

[a] Instituto Pirenaico de Ecología (IPE-CSIC), Avda. Montañana 1005, Zaragoza 50192, Spain
[b] Scuola di Scienze Agrarie, Forestali, Alimentari e Ambientali, Università della Basilicata, Viale dell'Ateneo Lucano 10, Potenza 85100, Italy
[c] Laboratory of Tree-Ring Research, University of Arizona, Tucson, AZ, USA
[d] Area of Ecology, Faculty of Biology, University of Salamanca, Salamanca, Spain

ARTICLE INFO

Keywords:
Celtis australis
Hydraulic diameter
Pistacia terebinthus
Wood anatomy

ABSTRACT

Drought-tolerant tree species with high growth rates and a good capacity for carbon storage in woody tissues (dense wood) are searched for due to aridification. Deciduous, ring-porous tree and shrub species could show such drought tolerance and growth traits, thus representing good candidates for climate-smart rewilding. However, we still do not know the long-term growth rates of these species and how they respond to drought, particularly in climate change hotspots such as the Mediterranean Basin. We analysed these issues at the site and individual levels in two ring-porous, deciduous species (*Pistacia terebinthus*, *Celtis australis*) using dendroecology and wood anatomy. The ring width, earlywood vessel diameter, vessel density (VD) and area (%) were measured in two focal sites, one per species, and then growth data were compared with two secondary sites to test if site-to-site synchrony changed through time. Ring-width indices (RWI) and the hydraulic diameter (*Dh*) of earlywood were calculated. Growth rates (ring width), *Dh* and vessel area were higher in *C. australis* (1.03−2.26 mm, 269 μm, 33.9 %) than in *P. terebinthus* (0.57−0.72 mm, 146 μm, 21.5 %). Consequently, VD was higher in *P. terebinthus* than in *C. australis* (104 vs. 61 vessels mm^{-2}). The ring width and *Dh* were more coupled in *P. terebinthus* ($r = 0.43$) than in *C. australis* ($r = 0.32$). RWI series of the focal and secondary sites have been synchronized since the 1990s as temperatures rose. Precipitation during the growing season (May, June) enhanced growth and VD of both species. *P. terebinthus* was more responsive to a drought index than *C. australis*. The two study species show high growth rates and tolerate drought being thus suitable candidates for climate-smart rewilding.

1. Introduction

Drought is becoming a major constraint of forest productivity and tree growth worldwide (Babst et al., 2019). The frequency and severity of droughts are expected to increase in climate-warming hotspots such as the Iberian Peninsula (García-Valdecasas Ojeda et al., 2021). More frequent hotter droughts will have negative impact on forests making them more vulnerable to further stress, reducing their resilience and increasing the mortality risk of major tree groups such as pines or oaks (Gazol et al., 2020). Therefore, there is a great interest in broadleaf minor tree species which could show higher drought tolerance under warmer climate scenarios than some abundant tree species. Some studies have dealt with this issue in temperate central European tree species (Kunz et al., 2018; Fuchs et al., 2021), but there are still few data on Mediterranean tree species, except in particular cases such as the service tree (*Sorbus domestica* L.; see Camarero et al., 2023).

Minor, hardwood, broadleaf species with high-quality timber (dense wood) and fast growth rates could contribute to climate-smart rewilding through carbon uptake and storage under more arid conditions. This could be the case of the Mediterranean hackberry (*Celtis australis* L., Ulmaceae) and the terebinth (*Pistacia terebinthus* L., Anacardiaceae), two winter-deciduous tree and tree-to-shrub species which form ring-porous wood and are native to the Mediterranean Basin (Magni and Caudullo, 2016). Despite their Circum-Mediterranean distribution (Fig. 1), both

* Corresponding author.
E-mail addresses: jjcamarero@ipe.csic.es (J.J. Camarero), michele.colangelo@unibas.it (M. Colangelo), agazol@ipe.csic.es (A. Gazol), cvaleriano@ipe.csic.es (C. Valeriano), mortegam09@gmail.com (M.A. Ortega), fsilla@usal.es (F. Silla).

https://doi.org/10.1016/j.foreco.2024.122282
Received 19 June 2024; Received in revised form 3 September 2024; Accepted 4 September 2024
Available online 7 September 2024

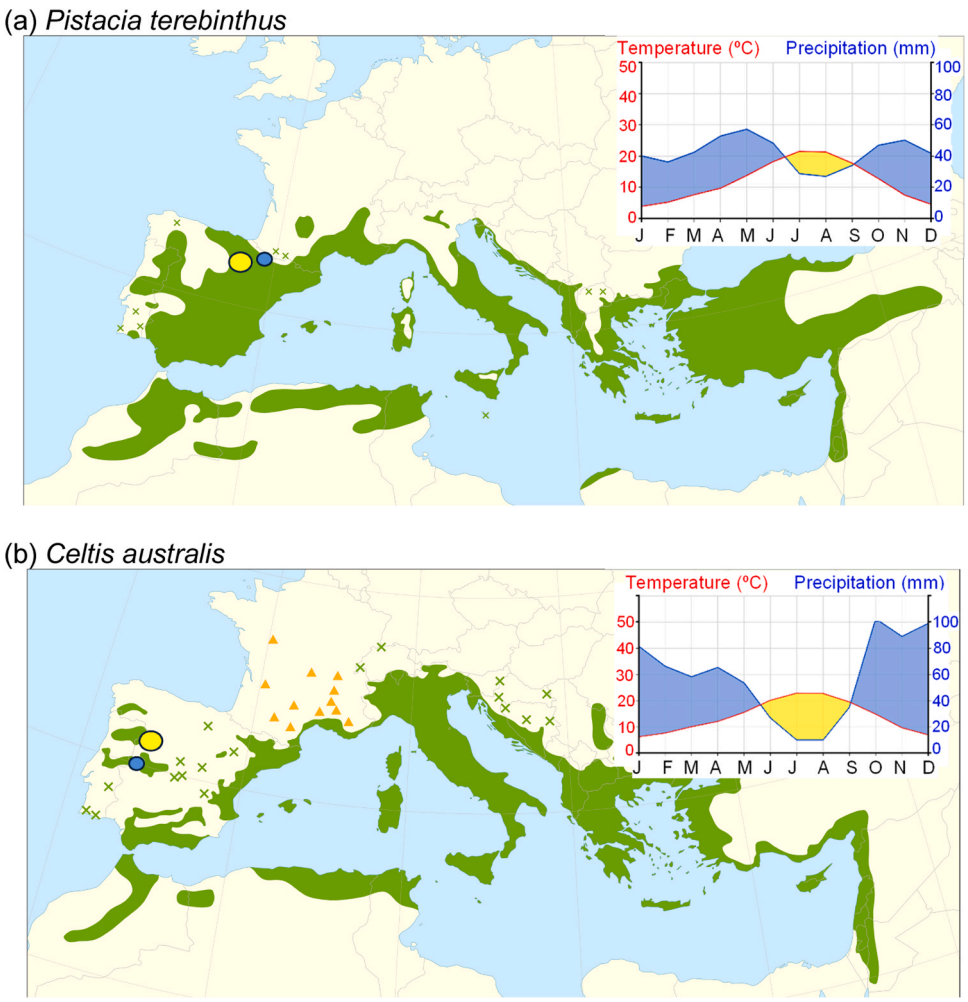

Fig. 1. Climate diagrams of the focal sites and distribution maps of the two study species in the Mediterranean Basin: (a) *Pistacia terebinthus*; (b) *Celtis australis*. The yellow and blue symbols show the approximate location of the focal and secondary study sites in Spain, respectively. Green areas and crosses indicate the native distribution area, whereas yellow triangles correspond to introduced and naturalized populations (modified from Caudullo et al., 2017).

genera can be considered of tropical origin (Axelrod, 1958; Palamarev, 1989). The two study species show an early aboveground phenology and start forming shoots and new leaves from March to May, whereas their leaves are shed from October to December (Castro-Díez and Montserrat-Martí, 1998).

Ring porosity and deciduousness are two traits common in areas with seasonal climates and they are often linked as shown in analyses of European temperate trees with 94 % of the ring-porous species being also deciduous (Boura and De Franceschi, 2007). However, only about 4 % of tree species have ring-porous wood worldwide, albeit 18 % of tree species in temperate regions form ring-porous wood. Ring porosity is considered an adaptation to seasonal climates by showing a trade-off between vessel diameter and vessel density along the annual ring (Gilbert, 1940; Carlquist, 2001). In these woody plant species, the earlywood is characterized by vessels with large lumen area which account for most hydraulic conductivity (Ellmore and Ewers, 1985). These vessels are rapidly formed for water transport to expanding buds (Kitin and Funada, 2016) and their formation requires the mobilization of stored carbon (Barbaroux and Bréda, 2002), but they become embolised since conduit diameter is correlated with vulnerability to freeze- and drought-induced embolism (Sperry et al., 1994). Latewood vessels provide safety during the late growing season and allow conducting water before the earlywood vessels are formed in the following spring (Kitin and Funada, 2016).

In the case of Mediterranean and temperate ring-porous species, they have to withstand unfavorable climatic conditions for growth during summer (drought) and autumn-winter (cold) (Mitrakos, 1980). Consequently, they inhabit sites with good soil water availability and often show high growth rates and early phenology, i.e. they start growing earlier than congeneric evergreen species (Montserrat-Martí et al., 2009). These species can be considered as water-spender because they display anisohydric behavior by maintaining both open stomata and high photosynthesis rates (Kolb and Stone, 2000; McCulloh et al., 2010; Klein, 2014). They often rely on deep soil water sources (Ripullone et al., 2020) and show a high hydraulic capacitance and small variations in sap flux during drought (Yi et al., 2017; Bader et al., 2022).

The commented phenological and ecophysiological features confer ring-porous species drought tolerance. To have a long-term assessment of their growth rates and to quantify how they change in response to climate and water shortage we need retrospective approaches. Tree-ring data and earlywood anatomy allow reconstructing radial growth rates and responses to climate variability in ring-porous species because the series of earlywood vessel variables (e.g., lumen diameter) usually exhibit a low common signal, but are strongly related to climate (García-González and Eckstein, 2003; Fonti and García-González, 2004; García-González et al., 2016). Here, we aim to assess: (i) the radial growth and earlywood anatomy patterns and (ii) the responses to climate variables and a drought index in two minor, ring-porous, deciduous Mediterranean species (*P. terebinthus*, *C. australis*). To achieve these aims we used dendroecology and quantitative wood anatomy and

Table 1
Geographical and structural features of sampled sites and trees. Values are means ± SE. Different letters indicate significant ($p < 0.05$) differences between sites within each species according to Mann-Whitney tests.

Variable	*Pistacia terebinthus*		*Celtis australis*	
	El Cajo[a]	Guara	Mieza[a]	Ciudad Rodrigo
Latitude N	41.948	42.241	41.166	40.740
Longitude W	1.903	0.049	6.712	6.663
Elevation (m a.s.l.)	641	942	325	560
Slope (º)	4	10	16	5
Other tree species	*Quercus ilex*	*Quercus ilex*	*Quercus suber*	*Quercus ilex*
Diameter at 1.3 m (cm)	21.6 ± 0.8	19.3 ± 0.5	31.1 ± 1.1	27.4 ± 3.8
Age at 1.3 m (years)	59 ± 1a	79 ± 4b	76 ± 2b	58 ± 1a
No. trees / No. cores	18 / 36	15 / 26	20 / 40	15 / 30
Tree-ring width (mm)	0.72 ± 0.05b	0.57 ± 0.03a	1.03 ± 0.03a	2.26 ± 0.24b

[a] Focal sites where wood anatomy was measured.

compared two focal (with growth and anatomy data) and two secondary sites (only with growth data) for each species in Spain. The focal and secondary sites were similar in climate and ecological conditions to determine if growth rates and climate-growth couplings are maintained in space. The general goal of the study is to evaluate the suitability of these two species to withstand warmer and drier climate conditions in southern Europe, where forests and shrublands are encroaching. We expect that the two species will show a high drought tolerance, thanks to their early aboveground phenology and deciduousness which allow them avoiding summer drought stress, and high growth rates due to their ring-porous wood providing large hydraulic conductivity in the early growing season. We also expect: (i) a strong coupling between growth rates and earlywood vessel diameter, which determines the potential hydraulic conductivity and impacts on water-gas exchange rates (Zanne et al., 2010), (ii) a significant influence of previous winter climate conditions on earlywood vessel diameter, and (iii) positive growth responses to spring precipitation given the early growth phenology of the study species.

2. Material and methods

2.1. Study sites

The two main or focal study sites are located in Northern (El Cajo, La Rioja province) and Western (Mieza, Salamanca province) Spain, respectively (Fig. 1). The two study species were sampled in each site (*P. terebinthus* in El Cajo, *C. australis* in Mieza) because they are relatively undisturbed since the 1970s and form large stands (0.5− 3.0 ha) with abundant mature individuals. In Mieza, *C. australis* forms one of the largest and best preserved populations of the species in Spain (Hernández Herrán, 1998). The secondary tree species abundant in El Cajo and Mieza sites are *Quercus ilex* L. and *Quercus suber* L., respectively. Some *P. terebinthus* individuals also appear in the Mieza site. Substrates are rocky and trees often appear growing in fissures or cracks. Soils are basic and acid in El Cajo and Mieza, respectively. In both sites, rivers or streams are located near the sampled stands (Añamaza river in El Cajo, and Duero river in Mieza) probably providing high air humidity levels in summer.

In addition to the two main or focal sites, two sites of *P. terebinthus* and *C. australis* were also sampled in Guara and Ciudad Rodrigo, respectively (Table 1). These additional sites were similar in climate, soil, tree size, and forest composition to the focal sites and were used to compare if site-to-site correlations of growth indices remained stable over time. The linear distance (142 km) between the two *P. terebinthus* sites (El Cajo and Guara) was larger than that (62 km) separating the two *C. australis* sites (Mieza and Ciudad Rodrigo).

Climate conditions in the main sites are Mediterranean characterized by dry summers, cool winters, and high year-to-year precipitation variability. In El Cajo, the mean annual temperature (MAT) is 12.4 ºC and the total annual precipitation (TAP) is 455 mm (data from Cabretón station, 41.99º N, 1.90º W, 513 m a.s.l., situated at 5 km northeast from the study site). In Mieza, the MAT is 15.5 ºC and the TAP is 671 mm (data from Salto de Aldeadávila station, 41.19º N, 6.69º W, 220 m a.s.l., located at 3 km north from the sampling site). Drought duration is longer in Mieza, but autumn precipitation is higher than in El Cajo. Climate conditions in the secondary sites are similar, but slightly warmer-drier in Guara (MAT, 14.0 ºC; TAP, 412 mm) than in El Cajo and slightly drier in Ciudad Rodrigo (MAT, 15.6 ºC; TAP, 622 mm) than in Mieza.

2.2. Field sampling

Sampling of two focal sites (El Cajo, Mieza) was done in winter 2020−2021, whilst the other two sites (Guara, Ciudad Rodrigo) were sampled in winter 2023−2024. The mean slope and elevation of each sampled site were recorded (Table 1). For sampling, a representative 1-ha large area was selected, and 15−20 mature, apparently healthy individuals per species and site were sampled. During sampling, we did not distinguish between males and females in the case of the diecious *P. terebinthus*, but a previous study found no differences in growth between the two genders (García-Barreda et al., 2022). The diameter at 1.3 m of sampled trees was measured using tapes. Then, two 5-mm cores at 1.3 m and perpendicular to the maximum slope were extracted from each individual using Pressler increment borers. The height of sampled individuals ranged 9−12 and 5−7 m in the case of *C. australis* and *P. terebinthus*, respectively.

2.3. Analysing tree-ring width and earlywood anatomy

Cores were air dried in the laboratory, glued to wooden mounts, and surfaced with progressively finer sandpapers for visualizing tree-ring boundaries (Fritts, 1976). Then, they were scanned at 2400 dpi resolution and visually cross-dated under a stereoscope. Ring widths were measured with a 0.001 mm resolution using scanned images and the CooRecorder-CDendro software (Maxwell and Larsson, 2021; Larsson and Larsson, 2022). The quality of cross-dating was checked using the COFECHA software which calculates moving correlations between individual series of ring-width values and the mean sites series (Holmes, 1983).

In the two focal sites (El Cajo, Mieza), the five trees showing highest correlations with the mean site series of ring-width indices were selected for each species to analyze their earlywood anatomy. One core from each tree was divided into pieces approximately 2–5 cm long. Then, cross-sections (thickness of 10−20 μm) were obtained using a sledge microtome (Gärtner and Nievergelt, 2010). Cross-sections were stained with safranin (1 %) and Astra blue (2 %), and fixed with Eukitt®. High-resolution images of the cross-sections were captured using an Olympus BH2 microscope equipped with an Olympus DP73 camera. The images were stitched with PT-Gui (New House Internet Services BV, Rotterdam, NL) to create one composite image for each sample. The images were analysed using the image analysis freeware ImageJ ver. 1.54i (Schneider et al., 2012), which provided the radial diameter and centroid position of each earlywood vessel within each cross-dated annual ring. The lower limit for vessel identification was set at a diameter of 20 μm. The vessel diameters were measured in a tangential window of 2 mm. Then, we calculated for each annual ring (Scholz et al., 2013): the minimum, mean, and maximum vessel diameters, the percentage of earlywood area occupied by vessels, and the vessel density (VD). Lastly, the hydraulic diameter (*Dh*) was calculated as the average of $\sum d^5/\sum d^4$, where d is the diameter of each earlywood vessel assuming a circular shape (Sperry et al., 1994). The mean series of each variable

were calculated for each site and species.

2.4. Climate data and drought index

We considered several temporal scales of climate data and the drought index (10 days, week, and month) to analyze growth and wood-anatomy responses to climate and drought severity at different temporal scales. Due to the lack of long, homogeneous climate datasets near the study sites we used 0.1°-gridded daily and monthly climate variables (Tmin, mean minimum temperatures; Tmax, mean maximum temperatures; prec, precipitation) from the E-OBS dataset ver. 29.0e (Cornes et al., 2018). In El Cajo site, 10-day mean minimum and maximum temperatures, or 10-day summed precipitation of the local weather station situated in Cabretón were compared with E-OBS interpolated data (period 2006–2020). In all cases, correlations between both datasets were significant ($p < 0.05$), albeit measured precipitation tended to be higher than interpolated precipitation (Fig. S1).

To assess changes in drought severity and duration, we used the multiscalar Standardized Precipitation-Evapotranspiration Index (SPEI), which accounts for the influences of temperature and precipitation on the cumulative water balance (Vicente–Serrano et al., 2010). The SPEI was calculated at 1-3-, 6-, 9-, and 12-month long scales. In the case of SPEI, weekly data (period 1980–2020) were retrieved from the Spanish 1.1-km^2-gridded dataset available at the webpage https://monitordesequia.csic.es (Vicente-Serrano et al., 2017). In all study sites, temperatures have significantly increased since 1950 (τ tests, $p < 0.05$), whereas precipitation decreased in the Mieza site (Fig. S2).

2.5. Processing tree-ring and wood-anatomical data

First, to have an accurate indicator of radial increment (Biondi and Qeadan, 2008), we transformed ring-width (RW) measures into basal area increment (BAI) assuming concentric growth and using the formula:

$$BAI = \pi (r_t^2 - r_{t-1}^2) \quad (1)$$

where r_t and r_{t-1} represent the width of the rings in the year t and t-1, respectively. Mean BAI series were calculated by averaging the BAI series of the individuals sampled in each site.

Second, the age of each individual at 1.3 m was obtained by counting the maximum number of annual rings from bark to pith. Third, to calculate climate– and SPEI–growth correlations individual ring-width (RW) series were detrended by fitting x-year cubic smoothing splines with a 50 % frequency response cut-off, where x was 2/3 of the mean series length (Cook and Peters, 1981). The measured ring-width values were divided by fitted values. The resulting series of dimensionless ring-width indices (RWI) were pre-whitened by fitting auto-regressive models, and bi-weight robust means were used to obtain site residual series or chronologies preserving annual to decadal variability (Fritts, 1976). A similar procedure was carried out with the *Dh* and VD series to remove trends due to tapering, i.e. the reduction of *Dh* in taller stems (Olson et al., 2018). This allowed removing size-related trends in ring-width and wood-anatomy data and emphasizing high-frequency variability.

2.6. Statistical analyses

Trends in annual climate variables were assessed using Mann-Kendall τ tests. Mann-Whitney tests were used to test for differences between species considering several variables (diameter, age at 1.3 m, tree-ring, and wood-anatomical variables). An ANCOVA test was used to compare the *Dh*–RW regressions' slopes of the two species. These regressions were fitted using log-transformed data and standardized major axis (SMA) (Warton et al., 2006).

Pearson correlations between climate variables or the SPEI and growth or wood-anatomical indices were calculated at 10-day and monthly temporal scales in the two focal sites. At monthly scale, correlations and response function analyses were performed to account for the multicollinearity between climate predictors (Fritts, 1976). In addition, climate–growth relationships were also calculated at monthly temporal scales in the secondary sites. Correlation and response function coefficients were obtained from the previous October to the current September. Site-to-site correlations of growth indices, i.e. by correlating the chronologies of focal and secondary sites, were calculated during the common period 1970–2020 using a 20-year moving Pearson correlation shifted year by year.

Lastly, we calculated several dendrochronological statistics for the common, best-replicated period (1964–2020 and 1964–2023 in the focal and secondary sites, respectively). This period was defined based on the values of the Expressed Population Signal (EPS). We considered the period with EPS $\geq$ 0.85 as the best-replicated one (Wigley et al., 1984). We also characterized the mean site chronologies by calculating: the mean ring-width values, the mean first-order autocorrelation of ring widths, which accounts for year-to-year persistence in growth, the mean sensitivity (MS), which measured relative changes in ring-width indices between consecutive rings, the correlation with mean sites series, and the EPS (Briffa and Jones, 1990). The internal coherence of each site series was measured by calculating the mean correlation between individual ring-width and anatomy series (rbar).

We used generalized additive mixed effect models (GAMM; Wood, 2017) to study the relationship of growth (BAI), hydraulic diameter (*Dh*), and vessel density (VD) as a function of climate variability and drought severity (SPEI) at the individual level, while accounting for age and size effects, in the two focal sites. We ran separate models for the focal sites of each species using as response variables either BAI, *Dh* or VD, and tree identity as random intercept. As explanatory variables fixed in all models, we considered tree age (from 1 to the age at coring date) and diameter (fixed value per individual) as smooth terms with default settings (Wood, 2003). As climatic variables, we considered the mean maximum and minimum temperatures and the precipitation for the growing season, i.e. from April to July. Additionally, we considered the 3-, 6-, 9- and 12-month long SPEI for June. BAI was log-transformed (log (x+1)) prior to the analyses. Models were compared based on the Akaike Information Criterion (AIC; Burnham and Anderson, 2002) but restricting the total number of variables included in the model to three and including smooth terms for age and dbh in all models. Thus, we tested one-by-one the capacity of each climatic variable. Then, the most parsimonious model, with the lowest AIC, of those containing no more than two of the above-mentioned factors was selected. We also calculated ΔAIC scores, i.e. differences between the model with the smallest AIC and each model, Akaike relative weights (w_i), which represent the relative likelihood of each fitted model, and adjusted R^2 values.

All statistical analyses were performed using the R statistical software (R Core Team, 2023). The dplR package was used to process dendrochronological data including the calculation of BAI and statistics (Bunn, 2008, 2010; Bunn et al., 2023). The treeclim R package was used to calculate the correlation and response functions between residual ring-width series and climate variables or SPEI (Zang and Biondi, 2015). The SMA was fitted using the smatr 3 package (Warton et al., 2012). The package MuMIn was used for model selection and estimation of adjusted R^2 values (Bartoń 2023).

3. Results

3.1. Radial growth and earlywood anatomy

In *P. terebinthus*, tree-ring width was higher in El Cajo than in Guara site (0.72 vs. 0.57 mm), where older trees (79 years) were sampled (Table 1). In *C. australis*, growth rates were lower in Mieza (1.03 mm) than in Ciudad Rodrigo (2.30 mm), where younger individuals were sampled.

Table 2
Growth and earlywood-anatomical features of the study species in the two focal sites (Cajo, Mieza) considering the common period 1980–2020. Earlywood anatomy was measured in five trees of each species. EPS is the Expressed Population Signal and *Dh* is the hydraulic diameter. Values are means ± SE. Different letters indicate significant ($p < 0.05$) differences between species according to Mann-Whitney tests.

Type of analyses	Variable	*Pistacia terebinthus*	*Celtis australis*
Dendrochronology	First-order autocorrelation	0.73 ± 0.02a	0.85 ± 0.01b
	Mean sensitivity	0.31 ± 0.01b	0.25 ± 0.01a
	Correlation with master series	0.43 ± 0.02a	0.56 ± 0.02b
	Period with EPS > 0.85	1964–2020	1947–2020
Earlywood anatomy	*Dh* (μm)	145.80 ± 1.39a	268.93 ± 3.47b
	Mean vessel diameter (μm)	43.21 ± 0.43a	53.21 ± 0.59b
	Vessel area (%)	21.52 ± 0.52a	33.87 ± 0.80b
	Vessel density (No. mm^{-2})	104.35 ± 2.94b	61.49 ± 1.28a

Regarding the ring-width data of the two focal sites, the first-order autocorrelation and correlation with the master series were lower in *P. terebinthus* than in *C. australis*, but the mean sensitivity was higher in the first species (Table 2). The mean BAI was higher in *C. australis* than in *P. terebinthus* (mean ± SE, 10.1 ± 0.4 vs. 2.2 ± 0.1 cm^2 yr^{-1}, $p < 0.001$; Fig. 2). The mean vessel diameter, the *Dh* (269 vs. 146 μm) and the percent vessel area were higher in *C. australis* than in *P. terebinthus*, whereas vessel density was higher in *P. terebinthus* (Figs. 2 and 3).

As expected, the coherence between series, measured as the mean correlation between indexed individual series (rbar), was much lower ($p < 0.001$) in the case of wood-anatomical variables (e.g., it ranged 0.14−0.16 in the case of *Dh* vs. 0.41−0.54 in the case of RWI) than in the case of ring-width (Table S1). Both RWI and VD series were positively correlated in the two species. The rbar values of RWIs and vessel diameter were higher in *C. australis* than in *P. terebinthus*. The RWI mean series of both species were positively and negatively related to the VD and MVA series, respectively (Table S2). In *P. terebinthus*, the series of RWI and maximum vessel diameter were positively correlated. Considering individual series and annual values, the slopes of the *Dh*−RW regressions did not significantly differ between species ($F = 2.22$, $p = 0.14$; Fig. 4).

Only the two RWI series of the nearby *C. australis* sites showed a positive and significant correlation (Fig. S3), albeit the series of the *P. terebinthus* and *C. australis* focal sites showed an almost significant correlation ($r = 0.20$, $p = 0.08$; Fig. 2). Interestingly, the RWI series of the focal and secondary sites are becoming increasingly synchronized since the 1995 and 1990 in *P. terebinthus* and *C. australis*, respectively, suggesting a stronger influence of regional climate conditions (Fig. S4).

3.2. Responses of growth and earlywood anatomy to climate and the drought index at the site level

In the case of *P. terebinthus*, growth indices (RWI) increased in response to high precipitation in the current June, high minimum temperatures in the previous October, and current April (Fig. 5).

The *Dh* increased in response to wet February conditions and high temperatures in June. High maximum temperatures in January and wet June conditions enhanced VD. In the case of *C. australis*, cool and wet conditions in the previous November and wet conditions in the current May enhanced growth, whereas wet conditions in March decreased *Dh* (Fig. 6). High minimum temperatures in February reduced VD. The climate−growth relationships in the secondary sites were similar to those of focal sites with *P. terebinthus* growth increasing in response to warmer April and wetter June conditions in Guara, and *C. australis* growth increasing in response to wet May and cool June conditions in Ciudad Rodrigo (Fig. S5).

The aforementioned results were based on monthly climate variables, whereas at 10-day resolution we found that *P. terebinthus* RWIs decreased as maximum temperatures increased from late June to early July and as early April and early June precipitation decreased, whereas the minimum vessel diameter increased as cumulative precipitation from late January to early February did (Figs. S6 and S7). In contrast, *Dh* decreased as mid-January precipitation increased. Mean vessel area decreased in response to warm February conditions, and, consequently, VD increased. In *C. australis*, the positive effect of precipitation on RWI was found in late May, and the negative effect on *Dh* correspond to high precipitation in early March (Fig. S8). Warm conditions in late March increased the minimum vessel diameter, and wet-cool conditions in April enhanced the mean vessel area. The negative impact of minimum temperatures on *C. australis* VD was detected in late February.

The correlations with the SPEI showed that growth decreased in response to dry conditions from May to September, particularly in the case of *P. terebinthus*, corresponding to 9-month long SPEI values (Fig. 7).

High 1-month SPEI values in March (wet conditions) decreased *Dh* in *C. australis*, whereas VD in *P. terebinthus* decreased in response to long droughts ending in the late growing season.

3.3. Responses of growth and earlywood anatomy to climate and the drought index at the individual level

According to the GAMMs fitted at the individual level, BAI depended on age and diameter, whereas earlywood anatomy only depended on age (Fig. S9, Table 3). The BAI and VD of *P. terebinthus* and *C. australis* were enhanced by high precipitation in May and June with high R^2 values in the case of BAI for both species and also in the case of VD for *C. australis*

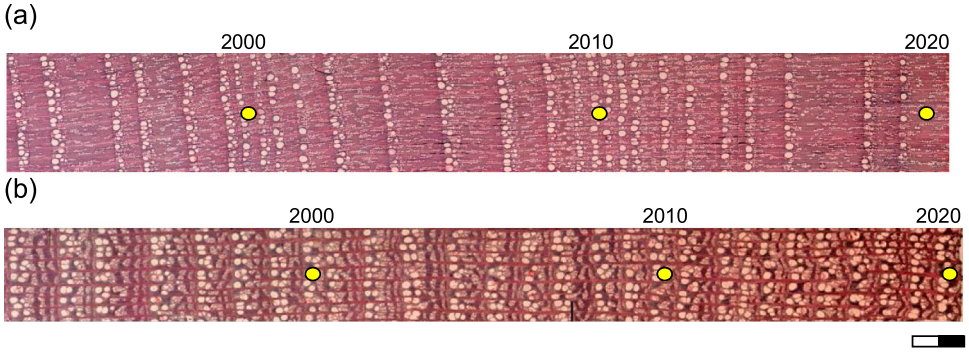

Fig. 2. Cross-sections of (a) *Pistacia terebinthus* and (b) *Celtis australis* sampled in the focal sites. In both cases, rings correspond to the period 1994−2020. Yellow dots indicate the rings formed in years 2000, 2010, and 2020. The scale bar measures 1 mm.

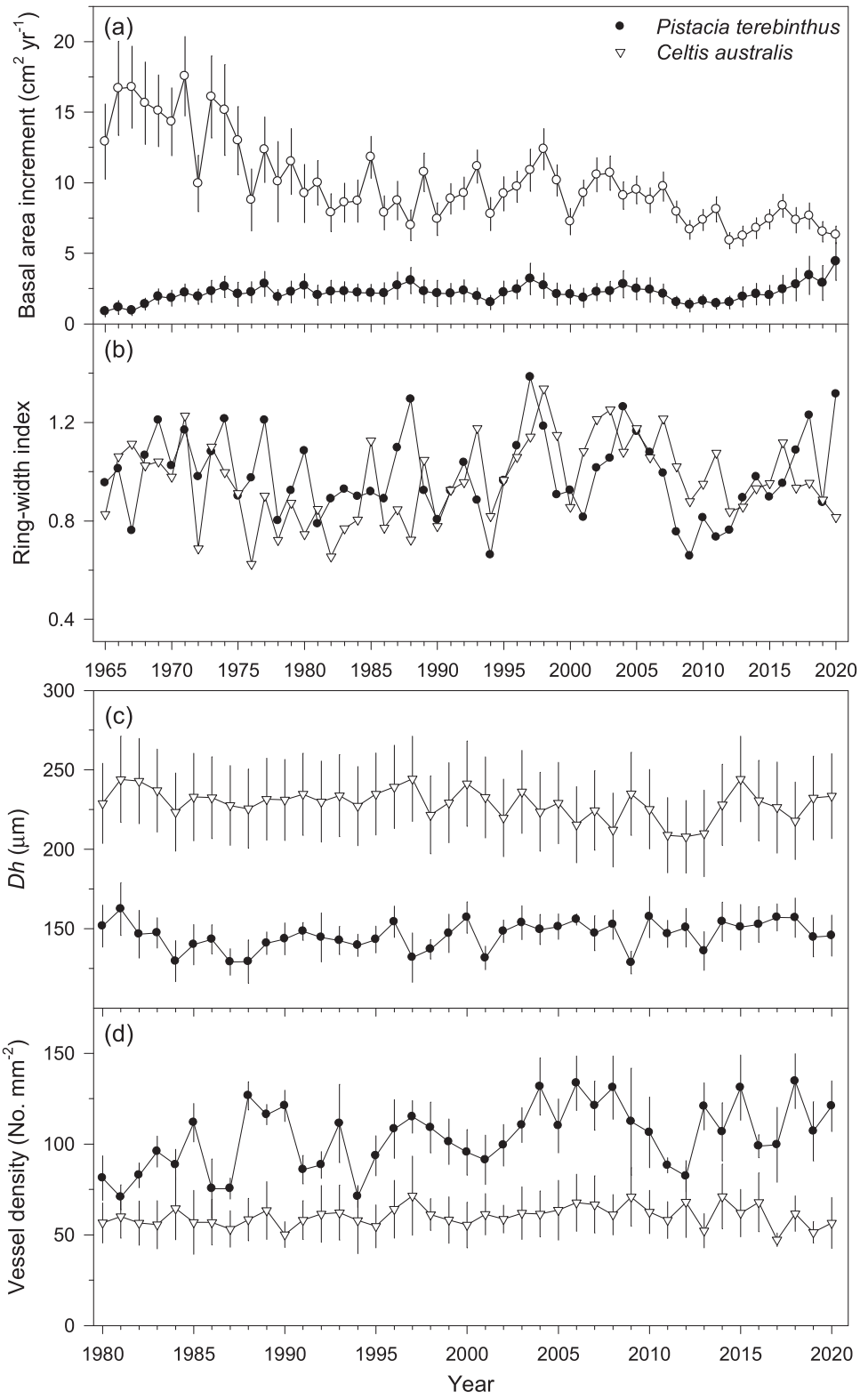

Fig. 3. Growth rates (a, basal area increment; ring-width indices) and earlywood anatomical variables (c, *Dh*, hydraulic diameter; d, vessel density) of the two ring-porous study species measured in the focal sites. Values are means ± SE. The best-replicated periods are shown.

(Table 3). Elevated minimum temperatures in June and July enhanced *Dh* in *P. terebinthus* and *C. australis*, respectively, with a high R^2 value in *P. terebinthus*.

4. Discussion

The growth rate and the earlywood vessel density (VD) of the study species depended on spring precipitation which agrees with their early phenology (Castro-Díez and Montserrat-Martí, 1998). Further, these findings concur with previous studies (Garfi, 2000; Camarero and

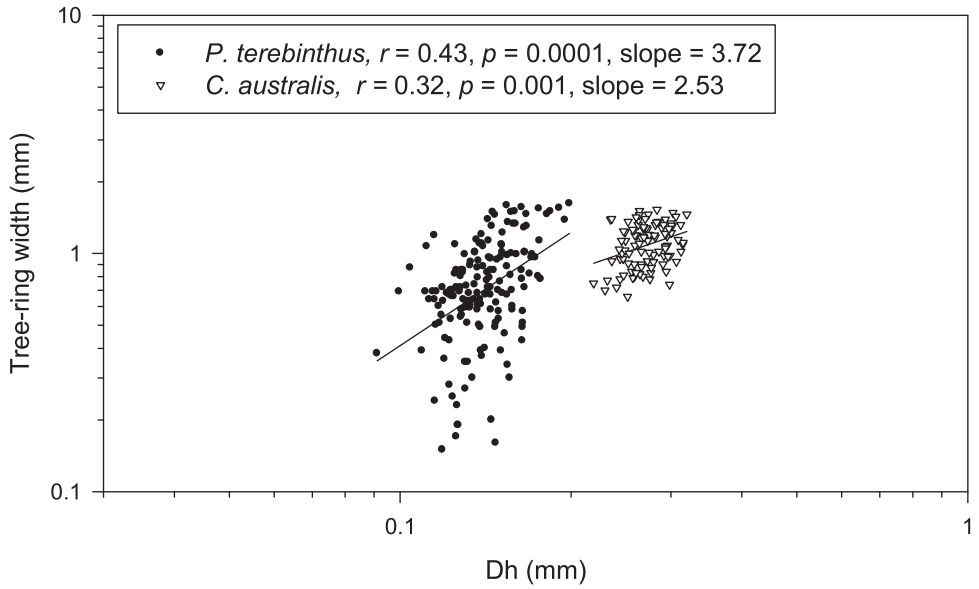

Fig. 4. Relationships found between log-transformed hydraulic diameter (*Dh*) and tree-ring width in *Pistacia terebinthus* (black symbols) and *Celtis australis* (white symbols) in the focal sites. Pearson correlation coefficients, associated probability levels, and slopes are shown.

Rubio-Cuadrado, 2020). These winter-deciduous Mediterranean species show a high growth rate from spring to early summer which allows them to avoid the cumulative water shortage of late summer. Ecologically, they are more similar to winter-deciduous Mediterranean oaks (e.g., *Quercus faginea* Lam; Corcuera et al., 2004). In contrast, coexisting evergreen, diffuse-porous species such as *Q. ilex* better withstand summer drought and can grow in spring and also in late summer and autumn if climate conditions are favorable (Montserrat-Martí et al., 2009; Campelo et al., 2018). Therefore, if winter-spring conditions become cooler and wetter, there could be some local replacement of dominant oak species such as *Q. ilex*. However, such substitution will probably be local and restricted to mesic sites with seasonally wet soils because the two study species rarely form large populations due to the scattered dispersal of their seeds by birds, among other factors.

Both study species showed a positive relationship between *Dh* and tree-ring width, as expected, which was stronger in *P. terebinthus*, the species forming more earlywood vessels but with smaller *Dh*. Such dependence of growth on the hydraulic conductivity in *P. terebinthus* may be explained by the formation of abundant earlywood vessels of similar diameter, whereas bigger vessels would be more important for *C. australis* growth.

Regarding the influence of previous winter climate conditions on earlywood *Dh*, the hypothesis was supported but results in the two species were contrasting because *Dh* increased in response to February precipitation and June temperatures in *P. terebinthus*, suggesting a long season of earlywood formation, but decreased in response to cool-wet March conditions in *C. australis*. Furthermore, the analyses at the individual scale showed that climate, mainly June temperature, accounted for more *Dh* variability in the case of *P. terebinthus*, but more growth (BAI) and VD variability in the case of *C. australis* with a higher importance of May precipitation. This difference reflects the tighter coupling between June growing conditions, *Dh* and growth in *P. terebinthus*, indicating that a previous wet February and cool June conditions contribute to the enlargement of vessels and wood production. In *C. australis*, the formation of abundant earlywood vessels and growth depend more on May rainfall suggesting a high dependence of cambium activity and cell turgor to produce bigger vessels contributing to hydraulic conductivity as leaves and the stem enlarge.

A more efficient stem water transport is expected to favor tree radial growth (Zanne et al., 2010; Hietz et al., 2017). However, an inverse relationship was found between radial growth and *Dh* in the ring-porous species *Lagerstroemia speciosa* which grows in tropical moist Asian forests (Islam et al., 2018). A decrease in *Dh* can be related to a higher potential hydraulic conductivity linked to wetter conditions and improved radial growth (Pérez-de-Lis et al., 2018). In contrast, trees respond to soil (low SPEI) or atmospheric drought (high VPD) by producing more small vessels to reduce the risk of xylem cavitation and reduce maximum vessel diameters to keep hydraulic efficiency (Sperry et al., 2008; Hacke et al., 2017). In addition, climate conditions of the previous autumn and winter, have been shown to affect wood anatomy and growth in ring-porous tree species of temperate (García-González and Eckstein, 2003), Mediterranean (Alla and Camarero, 2012), and tropical (Islam et al., 2019) biomes. These lagged responses could be explained by carryover effects due to the production, storage or consumption of non-structural carbohydrates in the prior year which are used to form the new earlywood vessels the following growing season (Pérez-de-Lis et al., 2018).

Our results on earlywood anatomy concur with other studies on Mediterranean deciduous ring-porous tree species, mainly oaks (Corcuera et al., 2004, 2006; Gea-Izquierdo et al., 2012; Rita et al., 2016; Castagneri et al., 2017; Martínez-Sancho et al., 2017). However, our findings are original because they deal with minor, understudied species which may be suitable for climate smart rewilding. At least two reasons support their suitability to tolerate warmer and drier climate conditions. First, several oak species have shown canopy dieback and elevated mortality rates in response to severe droughts which reduced growth, particularly latewood production, impairing hydraulic safety in summer (Corcuera et al., 2004; Camarero et al., 2016), making necessary the search of other drought-tolerant tree and shrub species (Camarero et al., 2023). Second, the other Mediterranean woody plant species showing deciduousness and ring-porous wood are mostly vines (e.g., *Clematis vitalba*), which are less suitable for planting in rural areas. Therefore, the two study species represent potential candidates for rewilding because they can face water shortage in seasonal dry environments. Interestingly, the study species presented pronounced growth responsiveness to drought and a high wood density suggesting a high stem hydraulic capacitance (Camarero, 2018).

A pattern that deserves further attention is the opposite BAI trends showed by the two species with an increase in *P. terebinthus* and a decrease in *C. australis* (Fig. 2). It has been suggested that shrubs are more capable to thrive in harsh environments due to anatomical and morphological strategies such as displaying multiple stems and having a

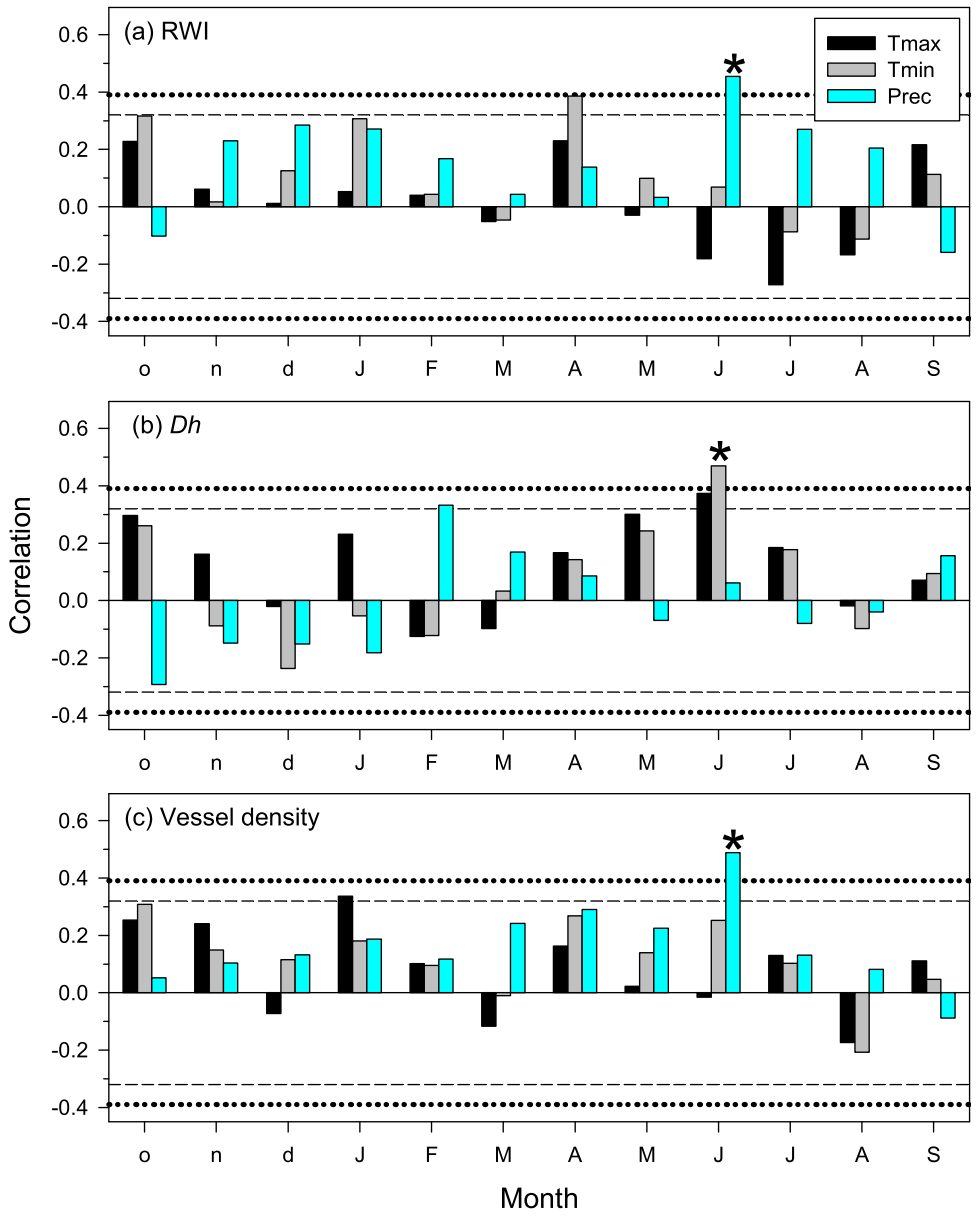

Fig. 5. Climate–growth and –anatomy relationships calculated for the *P. terebinthus* focal site using monthly climate variables (Tmax, mean maximum temperature; Tmin, mean minimum temperature; Prec, precipitation). The horizontal dashed and dotted lines show the 0.05 and 0.01 significance levels, respectively. Correlations were calculated from October of the previous year (months abbreviated by lowercase letters) to September of the current year (months abbreviated by uppercase letters). Asterisks indicate significant response coefficients.

lower mean vessel area but a larger vessel density (Götmark et al., 2016). Our results confirm these anatomical differences between *P. terebinthus* and *C. australis* (Table 2). Thus, despite presenting lower growth rates the capacity of *P. terebinthus* to display positive growth trends might suggest its ability to better tolerate drought than *C. australis*. These results are not confirmed by the climate-growth relationships (Fig. 7) because correlations with the drought index are in general higher in *P. terebinthus*. However, mixed models suggest a higher dependency of *C. australis* on May precipitation, whilst *P. terebinthus* depends on June precipitation (Table 3). The first species was sampled in sites located near river or streams that might provide high air humidity levels in summer. This might reflect the capacity of *P. terebinthus* to obtain water from deep sources which might be an advantage in a drier climate. In any case, further research might be required if this positive growth trend is the consequence of climate factors or simply a reflection of the phenology of shrub growth.

High late-winter to early-spring precipitation was related to larger *Dh* in *P. terebinthus*, but the opposite relationship was observed in *C. australis*. In the case of Mediterranean ring-porous oaks, drought was also associated with smaller earlywood vessels but higher VD (Corcuera et al., 2004; Gea-Izquierdo et al., 2012), as in *P. terebinthus*, suggesting that vessel enlargement was constrained by reduced turgor. In a Canadian temperate forest, drought induced the formation of fewer xylem vessels in ring-porous tree species (Buttó et al., 2021). This could be the case of *C. australis* if dry March conditions lead to the formation of larger but fewer vessels because of reduced cambial activity but high vessel enlargement rate.

It could be expected that the study species avoid dehydration through a reduction in water loss (deciduousness) or through deep water uptake (phreatophyte) (Volaire, 2018). To the best of our knowledge, there is no study on water uptake at different soil depths inferred from H and O isotopes in the two study species, but close species such as *Celtis reticulata* are considered phreatophytes (Robinson, 1958). Both species tend to grow near permanent or ephemeral streams or in valley bottoms

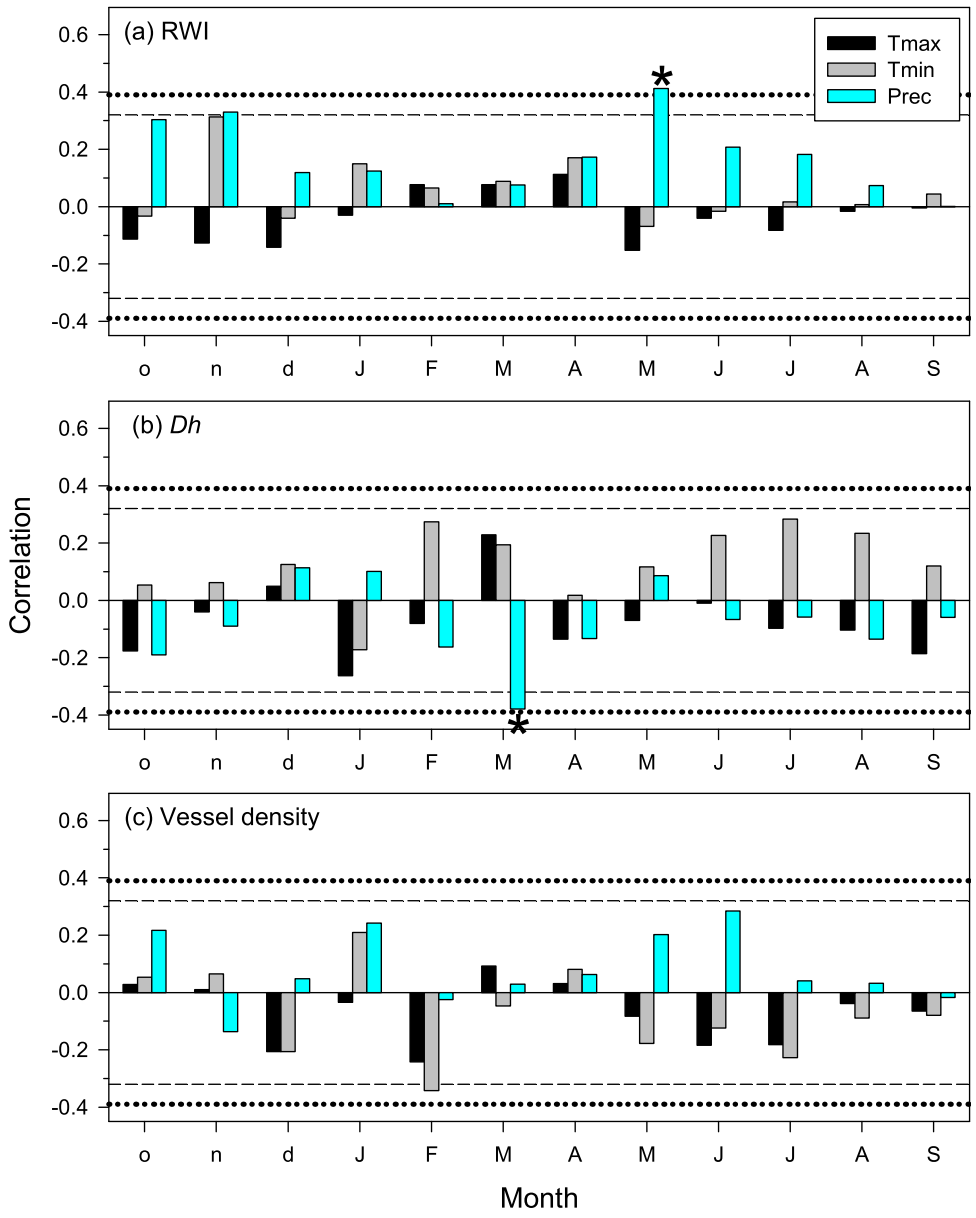

Fig. 6. Climate–growth and –anatomy relationships calculated for the *C. australis* focal site using monthly climate variables (Tmax, mean maximum temperature; Tmin, mean minimum temperature; Prec, precipitation). The horizontal dashed and dotted lines show the 0.05 and 0.01 significance levels, respectively. Correlations were calculated from October of the previous year (months abbreviated by lowercase letters) to September of the current year (months abbreviated by uppercase letters). Asterisks indicate significant response coefficients.

with well-drained soils suggesting they may use shallow and deep soil water sources. Nevertheless, summer drought increased the intrinsic water-use efficiency in both species confirming their responsiveness to water shortage (Camarero et al., 2018; García-Barreda et al., 2022). A caveat can be mentioned in the case of the diecious *P. terebinthus*, because males showed lower iWUE during dry years than females which could be related to different reproductive efforts (García-Barreda et al., 2022). However, we could not determine the sex of all sampled *P. terebinthus* individuals.

From a management point of view, these species could be planted as overstory (*C. australis*) or understory species (*P. terebinthus*) in Mediterranean pine plantations. Furthermore, their presence and dominance could be enhanced in favorable wet locations near streams, tracks or roads as major tree and shrub species. In addition, its deciduous leaf habit probably improves litter and soil quality as compared with stands dominated by co-occurring evergreen species (e.g., *Q. ilex*, *Pistacia lentiscus*). Lastly, its fruits and seeds will attract mammal, bird and insect species and increase biodiversity (Herrera, 1995).

5. Conclusions

To conclude, the winter-deciduous, ring-porous *P. terebinthus* and *C. australis* are suitable species for climate smart rewilding because of their high growth rates and drought tolerance. Their early aboveground phenology allows them avoiding Mediterranean summer drought stress. Moreover, their high wood density makes them good candidates for carbon sequestration under seasonal dry conditions. Finally, their different growth forms as trees (*C. australis*, *P. terebinthus*) or shrubs (*P. terebinthus*) would allow them forming different communities (forests, shrublands) modulating their responses to regional and local climate conditions as a function of site aridity (Gazol et al., 2024).

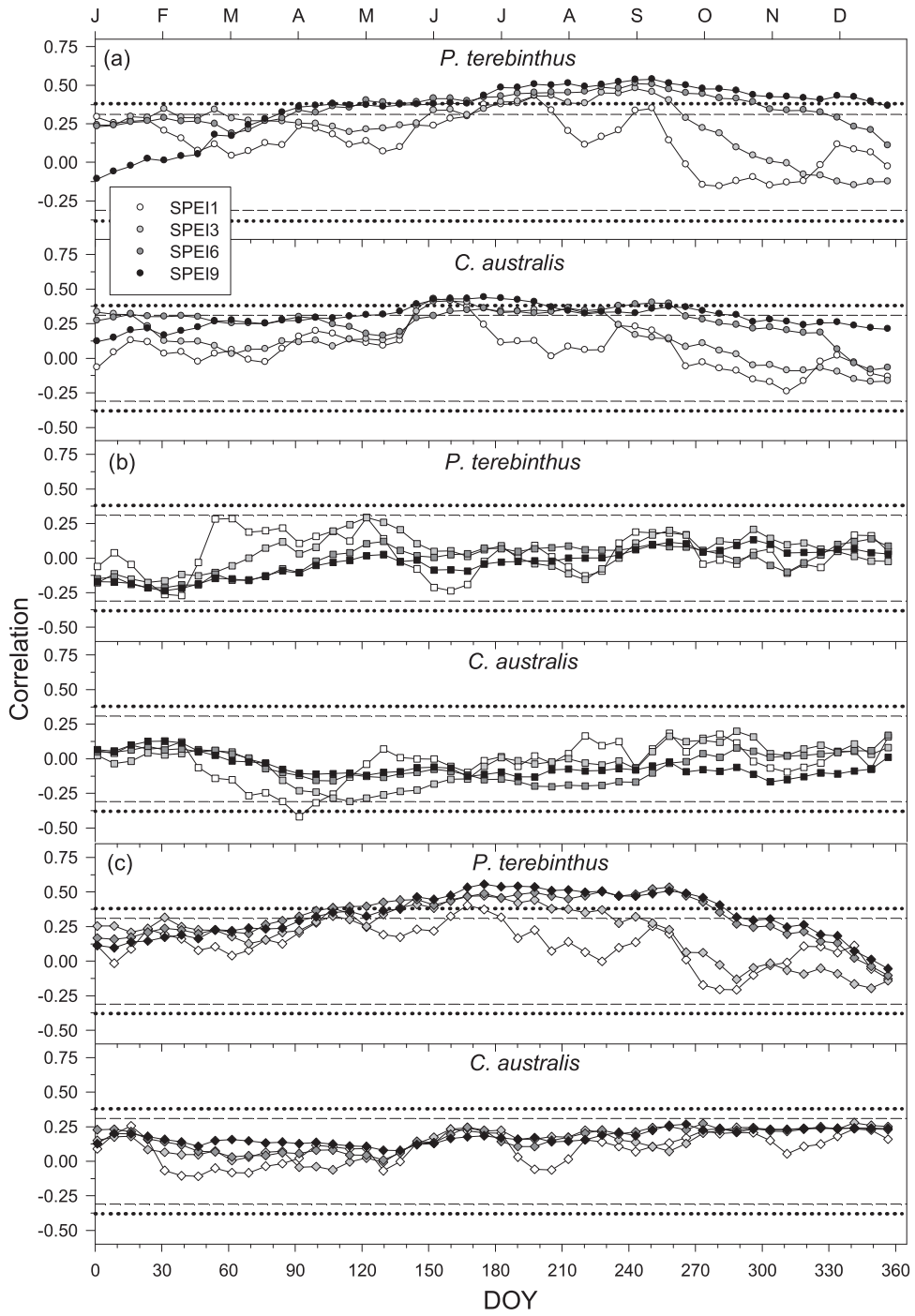

Fig. 7. Relationships between the weekly SPEI drought index and growth rates (a, RWI, ring-width indices) or wood-anatomical variables (b, *Dh*, hydraulic diameter; c, VD, vessel density) in the focal sites. Values are Pearson correlations calculated considering 10-day periods in *P. terebinthus* and *C. australis*. The SPEI was calculated for 1- (SPE1), 3- (SPE3), 6- (SPE6) and 9-month (SPE9) long periods. The horizontal dashed and dotted lines show the 0.05 and 0.01 significance levels, respectively.

CRediT authorship contribution statement

Antonio Gazol: Writing – review & editing, Validation, Supervision, Software, Resources, Project administration, Methodology, Investigation, Funding acquisition, Formal analysis, Conceptualization. **Michele Colangelo:** Writing – review & editing, Visualization, Methodology, Investigation, Formal analysis, Data curation. **J. Julio Camarero:** Writing – original draft, Visualization, Validation, Supervision, Software, Resources, Methodology, Investigation, Funding acquisition, Formal analysis, Data curation, Conceptualization. **Fernando Silla:** Writing – review & editing, Validation, Supervision, Resources, Methodology, Investigation, Data curation. **Miguel Angel Ortega:** Writing – review & editing, Methodology, Investigation, Formal analysis, Data curation, Conceptualization. **Cristina Valeriano:** Writing – review & editing, Validation, Supervision, Software, Resources, Methodology, Investigation, Formal analysis, Data curation, Conceptualization.

Declaration of Competing Interest

The authors declare that they have no known competing financial interests or personal relationships that could have appeared to influence

Table 3
Summary of the statistics of GAMMs fitted to basal area increment (BAI), hydraulic diameter (*Dh*), and vessel density (VD). The three best fitted models are shown for each variable and species. Climate variables are abbreviated by TN (mean minimum temperatures), TX (mean maximum temperatures), P (precipitation), SPEI drought index, and the number of the corresponding month. S(age) and s(dbh) are the smoothing terms of age and diameter, respectively.

Variable	Species	Intercept	s(Age)	s(dbh)	P4	P5	P6	P7	SPEI3	SPEI6	SPEI9	SPEI12	TN4	TN5	TN6	TN7	TX4	TX5	TX6	TX7	R^2	ΔAIC	w_i
BAI	*P. terebinthus*	0.418	+				0.022														0.677	0.001	0.693
		0.418	+	+				0.020													0.676	1.640	0.305
		0.418	+	+	+															−0.015	0.672	12.018	0.002
	C. australis	0.869	+	+		0.011															0.797	0.001	0.451
		0.869	+	+				−0.011													0.797	0.437	0.363
		0.869	+	+										−0.009							0.796	3.223	0.090
Dh	*P. terebinthus*	145.325	+												2.448						0.540	0.000	0.230
		145.318	+	+															1.906		0.537	1.377	0.115
		145.323	+						−1.949												0.536	1.836	0.092
	C. australis	275.173	+	+												3.464					0.201	0.000	0.335
		275.175	+	+											3.068						0.195	1.420	0.165
		275.184	+	+						−3.009											0.191	2.478	0.097
VD	*P. terebinthus*	104.348	+	+			8.956														0.228	0.000	0.983
		104.288	+	+		6.312															0.192	9.077	0.011
		104.322	+	+	5.535																0.183	11.187	0.004
	C. australis	72.765	+	+			1.614														0.781	0.000	0.147
		72.763	+	+		1.565															0.781	0.278	0.128
		72.760	+																−1.596		0.780	0.509	0.114

the work reported in this paper.

Data availability

Data will be made available on request.

Acknowledgments

We acknowledge the E-OBS dataset from the EU-FP6 project UERRA (https://www.uerra.eu) and the Copernicus Climate Change Service, and the data providers in the ECA&D project (https://www.ecad.eu). AG was supported by the "Ramón y Cajal" Program of the Spanish MICINN under Grant RyC2020–030647-I, and by CSIC under grant PIE-20223AT003. This research was funded by the Spanish Science, Innovation, and University Ministry (projects PID2021–123675OB-C43 and TED2021–129770B-C21).

Appendix A. Supporting information

Supplementary data associated with this article can be found in the online version at doi:10.1016/j.foreco.2024.122282.

References

Alla, A.Q., Camarero, J.J., 2012. Contrasting responses of radial growth and wood anatomy to climate in a Mediterranean ring-porous oak: implications for its future persistence or why the variance matters more than the mean. Eur. J. For. Res. 131, 1537–1550.
Axelrod, D.I., 1958. Evolution of the Madro-Tertiary geoflora. Bot. Rev. 24, 433–509.
Babst, F., Bouriaud, O., Poulter, B., Trouet, V., Girardin, M.P., Franck, D.C., 2019. Twentieth century redistribution in climatic drivers of global tree growth. Sci. Adv. 5, eeat4313.
Bader, M.K.-F., Scherrer, D., Zweifel, R., Körner, Ch, 2022. Less pronounced drought responses in ring-porous than in diffuse-porous temperate tree species. Agric. For. Meteorol. 327, 109184 https://doi.org/10.1016/j.agrformet.2022.109184.
Barbaroux, C., Bréda, N., 2002. Contrasting distribution and seasonal dynamics of carbohydrate reserves in stem wood of adult ring-porous sessile oak and diffuse-porous beech trees. Tree Physiol. 22, 1201–1210. https://doi.org/10.1093/treephys/22.17.1201.
Bartoń, K., 2023. _MuMIn: Multi-Model Inference_. R package version 1.47.5, <⟨https://CRAN.R-project.org/package=MuMIn⟩>
Biondi, F., Qeadan, F., 2008. A theory-driven approach to tree-ring standardization: defining the biological trend from expected basal area increment. Tree-Ring Res 64, 81–96.
Boura, A., De Franceschi, D., 2007. Is porous wood structure exclusive of deciduous trees? C. R. Palevol. 6, 385–391.
Briffa, K.R., Jones, P.D., 1990. Basic chronology statistics and assessment. In: Cook, E.R., Kairiukstis, L.A. (Eds.), Methods of Dendrochronology. Kluwer, Dordrecht, pp. 137–152.
Bunn, A.G., 2008. A dendrochronology program library in R (dplR). Dendrochronologia 26, 115–124.
Bunn, A.G., 2010. Statistical and visual crossdating in R using the dplR library. Dendrochronologia 28, 251–258.
Bunn, A.G., Korpela, M., Biondi, F., Campelo, F., Mérian, P., Qeadan, F., Zang, C., 2023. dplR: Dendrochronology Program Library in R. R package version 1.7.6, ⟨https://CRAN.R-project.org/package=dplR⟩.
Burnham, K.P., Anderson, D.R., 2002. Model Selection and Multimodel Inference: A Practical Information-theoretic Approach. Springer, New York.
Buttó, V., Millan, M., Rossi, S., Delagrange, S., 2021. Contrasting carbon allocation strategies of ring-porous and diffuse-porous species converge toward similar growth responses to drought. Front. Plant Sci. 12. DOI=10.3389/fpls.2021.760859.
Camarero, J.J., 2018. Linking functional traits and climate-growth relationships in Mediterranean species through wood density. IAWA J. 40, 215–240.
Camarero, J.J., Campelo, F., Sánchez-Sancho, J.A., Santana, J.C., 2023. Mediterranean service trees respond less to drought than oaks. For. Ecol. Manag. 541, 121070.
Camarero, J.J., Rubio-Cuadrado, A., 2020. Relating climate, drought and radial growth in broadleaf Mediterranean tree and shrub species: new approaches to quantify climate-growth relationships. Forests 11, 1250. https://doi.org/10.3390/f11121250.
Camarero, J.J., Sánchez-Salguero, R., Sangüesa-Barreda, G., Matías, L., 2018. Tree species from contrasting hydrological niches show divergent growth and water-use efficiency. Dendrochronologia 52, 87–95.
Camarero, J.J., Sangüesa-Barreda, G., Vergarechea, M., 2016. Prior height, growth, and wood anatomy differently predispose to drought-induced dieback in two Mediterranean oak species. Ann. For. Sci. 73, 341–351.
Campelo, F., Gutiérrez, E., Ribas, M., Sánchez-Salguero, R., Nabais, C., Camarero, J.J., 2018. The facultative bimodal growth pattern in *Quercus ilex* – a simple model to predict sub-seasonal and inter-annual growth. Dendrochronologia 49, 77–88.

Carlquist, S., 2001. Comparative Wood Anatomy, Systematic Ecological, and Evolutionary Aspects of Dicotyledon Wood. Springer, Berlin.
Castagneri, D., Regev, L., Boaretto, E., Carrer, M., 2017. Xylem anatomical traits reveal different strategies of two Mediterranean oaks to cope with drought and warming. Environ. Exp. Bot. 133, 128–138. https://doi.org/10.1016/j.envexpbot.2016.10.009.
Castro-Díez, P., Montserrat-Martí, G., 1998. Phenological pattern of fifteen Mediterranean phanaerophytes from *Quercus ilex* communities of NE-Spain. Plant Ecol. 139, 103–112.
Caudullo, G., Welk, E., San-Miguel-Ayanz, J., 2017. Chorological maps for the main European woody species. Data Brief. 12, 662–666. https://doi.org/10.1016/j.dib.2017.05.007.
Cook, E.R., Peters, K., 1981. The smoothing spline: a new approach to standardizing forest interior tree-ring width series for dendroclimatic studies. Tree-Ring Bull. 41, 45–53.
Corcuera, L., Camarero, J.J., Gil-Pelegrín, E., 2004. Effects of a severe drought on growth and wood anatomical properties of *Quercus faginea*. IAWA J. 25, 185–204. https://doi.org/10.1163/22941932-90000360.
Corcuera, L., Camarero, J.J., Sisó, S., Gil-Pelegrín, E., 2006. Radial-growth and wood-anatomical changes in overaged *Quercus pyrenaica* coppice stands: functional responses in a new Mediterranean landscape. Trees Struct. Funct. 20, 91–98. https://doi.org/10.1007/s00468-005-0016-4.
Cornes, R., van der Schrier, G., van den Besselaar, E.J.M., Jones, P.D., 2018. An ensemble version of the E-OBS temperature and precipitation datasets. J. Geophys. Res. Atmos. 123, 9391–9409. https://doi.org/10.1029/2017JD028200.
Ellmore, G.S., Ewers, F.W., 1985. Hydraulic conductivity in trunk xylem of elm, *Ulmus americana*. IAWA Bull. 6, 303–307.
Fonti, P., García-González, I., 2004. Suitability of chestnut earlywood vessel chronologies for ecological studies. N. Phytol. 163, 77–86.
Fritts, H.C., 1976. Tree Rings and Climate. Academic Press, London.
Fuchs, S., Schuldt, B., Leuschner, C., 2021. Identification of drought-tolerant tree species through climate sensitivity analysis of radial growth in Central European mixed broadleaf forests. For. Ecol. Manag. 494, 119287.
García-Barreda, S., Sangüesa-Barreda, G., García-González, M.D., Camarero, J.J., 2022. Sex and tree rings: females neither grow less nor are less water-use efficient than males in four dioecious tree species. Dendrochronologia 73, 125944.
García-González, I., Eckstein, D., 2003. Climatic signal of earlywood vessels of oak on a maritime site. Tree Physiol. 23, 497–504.
García-González, I., Souto-Herrero, M., Campelo, F., 2016. Ring-porosity and earlywood vessels: a review on extracting environmental information through time. IAWA J. 37, 295–314. https://doi.org/10.1163/22941932-20160135.
García-Valdecasas Ojeda, M., Gamiz-Fortis, S.R., Romero-Jiménez, E., Rosa-Canovas, J. J., Yeste, P., Castro-Díez, Y., Esteban-Parra, M.J., 2021. Projected changes in the Iberian Peninsula drought characteristics. Sci. Total Environ. 757, 143702.
Garfi, G., 2000. Climatic signal in tree–rings of *Quercus pubescens* s.l. and *Celtis australis* L. in South–eastern Sicily. Dendrochronologia 18, 41–51.
Gärtner, H., Nievergelt, D., 2010. The core–microtome: a new tool for surface preparation on core and time series analysis of varying cell parameters. Dendrochronologia 28, 85–92.
Gazol, A., Camarero, J.J., Sánchez-Salguero, R., Vicente-Serrano, S.M., Serra-Maluquer, X., et al., 2020. Drought legacies are short, prevail in dry conifer forests and depend on growth variability. J. Ecol. 108, 2473–2484. https://doi.org/10.1111/1365-2745.13435.
Gazol, A., Valeriano, C., Colangelo, M., Ibáñez, E., Valerio, M., Rubio-Cuadrado, A., Camarero, J.J., 2024. Growth of tree (*Pinus sylvestris*) and shrub (*Amelanchier ovalis*) species is constrained by drought with higher shrub sensitivity in dry sites. Sci. Total Environ. 918, 170539.
Gea-Izquierdo, G., Fonti, P., Cherubini, P., Martín-Benito, D., Chaar, H., Cañellas, I., 2012. Xylem hydraulic adjustment and growth response of *Quercus canariensis* Willd. to climatic variability. Tree Physiol. 32, 401–413. https://doi.org/10.1093/treephys/tps026.
Gilbert, S.G., 1940. Evolutionary significance of ring porosity in woody angiosperms. Bot. Gaz. 102, 105–120.
Götmark, F., Götmark, E., Jensen, A.M., 2016. Why be a shrub? A basic model and hypotheses for the adaptive values of a common growth form. Front. Plant Sci. 7, 203229.
Hacke, U.G., Spicer, R., Schreiber, S.G., Plavcová, L., 2017. An ecophysiological and developmental perspective on variation in vessel diameter. Plant, Cell Environ. 40, 831–845. https://doi.org/10.1111/pce.12777.
Hernández Herrán, R., 1998. El almez como especie dominante en una formación forestal. Ecol. ía 12, 285–292.
Herrera, C.M., 1995. Plant–vertebrate seed dispersal systems in the Mediterranean: Ecological, evolutionary, and historical determinants. Ann. Rev. Ecol. Syst. 26, 705–727.
Hietz, P., Rosner, S., Hietz-Seifert, U., Wright, S.J., 2017. Wood traits related to size and life history of trees in a Panamanian rainforest. New. Phytol. 213, 170–180. https://doi.org/10.1111/nph.14123.
Holmes, R.L., 1983. Program COFECHA user's manual. Laboratory of Tree–Ring Research, The University of Arizona, Tucson, USA.
Islam, M., Rahman, M., Bräuning, A., 2018. Long-term hydraulic adjustment of three tropical moist forest tree species to changing climate. Front. Plant Sci. 9, 1761. https://doi.org/10.3389/fpls.2018.01761.
Islam, M., Rahman, M., Bräuning, A., 2019. Long-term wood anatomical time series of two ecologically contrasting tropical tree species reveal differential hydraulic adjustment to climatic stress. Agric. For. Meteorol. 265, 412–423. https://doi.org/10.1016/j.agrformet.2018.11.037.
Kitin, P., Funada, R., 2016. Earlywood vessels in ring-porous trees become functional for water transport after bud burst and before the maturation of the current-year leaves. IAWA J. 37, 315–331. https://doi.org/10.1163/22941932-20160136.
Klein, T., 2014. The variability of stomatal sensitivity to leaf water potential across tree species indicates a continuum between isohydric and anisohydric behaviours. Funct. Ecol. 28, 1313–1320. https://doi.org/10.1111/1365-2435.12289.
Kolb, T.E., Stone, J.E., 2000. Differences in leaf gas exchange and water relations among species and tree sizes in an Arizona pine-oak forest. Tree Physiol. 20, 1–12.
Kunz, J., Löffler, G., Bauhus, J., 2018. Minor European broadleaved tree species are more drought-tolerant than *Fagus sylvatica* but not more tolerant than *Quercus petraea*. For. Ecol. Manag. 414, 15–27.
Larsson, L.A., Larsson, P.O., 2022. CDendro and CooRecorder (v. 9.8.1). Cybis Elektronik and Data AB, Saltsjöbaden, Sweden.
Magni, D., Caudullo, G., 2016. *Celtis australis* in Europe: distribution, habitat, usage and threats. In: European Atlas of Forest Tree Species, San-Miguel-Ayanz, J., de Rigo, D., Caudullo, G., Houston Durrant, T., Mauri, A., Eds., Publ. Off. EU, Luxembourg, e0145f9.
Martínez-Sancho, E., Dorado-Liñán, I., Heinrich, I., Helle, G., Menzel, A., Mencuccini, M., 2017. Xylem adjustment of sessile oak at its southern distribution limits. Tree Physiol. 37, 903–914. https://doi.org/10.1093/treephys/tpx036.
Maxwell, R.S., Larsson, L.-A., 2021. Measuring tree-ring widths using the CooRecorder software application. Dendrochronologia 67, 125841.
McCulloh, K., Sperry, J.S., Lachenbruch, B., Meinzer, F.C., Reich, P.B., Voelker, S., 2010. Moving water well: comparing hydraulic efficiency in twigs and trunks of coniferous, ring-porous, and diffuse-porous saplings from temperate and tropical forests. N. Phytol. 186, 439–450.
Mitrakos, K., 1980. A theory for mediterranean plant life. Oecol. Plant. 1, 245–252.
Montserrat-Martí, G., Camarero, J.J., Palacio, S., Pérez-Rontomé, C., Milla, R., Albuixech, J., Maestro, M., 2009. Summer-drought constrains the phenology and growth of two co-existing Mediterranean oaks with contrasting leaf habit: implications for their persistence and reproduction. Trees Struct. Funct. 23, 787–799.
Olson, M.E., Soriano, D., Rosell, J.A., Anfodillo, T., Donoghue, M.J., et al., 2018. Plant height and hydraulic vulnerability to drought and cold. Proc. Natl. Acad. Sci. USA 115, 7551–7556. https://doi.org/10.1073/pnas.1721728115.
Palamarev, E., 1989. Paleobotanical evidences of the Tertiary history and origin of the Mediterranean sclerophyll dendroflora. Plant Syst. Evol. 162, 93–107.
Pérez-de-Lis, G., Rozas, V., Vázquez-Ruiz, R.A., García-González, I., 2018. Do ring-porous oaks prioritize earlywood vessel efficiency over safety? Environmental effects on vessel diameter and tyloses formation. Agric. For. Meteorol. 248, 205–214. https://doi.org/10.1016/j.agrformet.2017.09.022.
R Core Team, 2023., R: A language and environment for statistical computing. R Foundation for Statistical Computing.
Ripullone, F., Camarero, J.J., Colangelo, M., Voltas, J., 2020. Variation in the access to deep soil water pools explains tree-to-tree differences in drought-triggered dieback of Mediterranean oaks. Tree Physiol. 40, 591–604.
Rita, A., Borghetti, M., Todaro, L., Saracino, A., 2016. Interpreting the climatic effects on xylem functional traits in two Mediterranean oak species: the role of extreme climatic events. Front. Plant Sci. 7, 1126. https://doi.org/10.3389/fpls.2016.01126.
Robinson, T.W., 1958. Phreatophytes. Geologial Survey Water-Supply Paper 1423. Washington, USA.
Schneider, C.A., Rasband, W.S., Eliceiri, K.W., 2012. NIH Image to ImageJ, 25 years of image analysis. Nat. Methods 9, 671–675.
Scholz, A., Klepsch, M., Karimi, Z., Jansen, S., 2013. How to quantify conduits in wood? Front. Plant Sci. 4, 1–11. https://doi.org/10.3389/fpls.2013.00056.
Sperry, J.S., Meinzer, F.C., McCulloh, K.A., 2008. Safety and efficiency conflicts in hydraulic architecture: scaling from tissues to trees. Plant, Cell Environ. 31, 632–645. https://doi.org/10.1111/j.1365-3040.2007.01765.x.
Sperry, J.S., Nichols, K.L., Sullivan, J.E.M., Eastlack, S.E., 1994. Xylem embolism in ring-porous, diffuse-porous, and coniferous trees in northern Utah and interior Alaska. Ecology 75, 1736–1752.
Vicente-Serrano, S.M., Tomas-Burguera, M., Beguería, S., Reig, F., Latorre, B., et al., 2017. A high resolution dataset of drought indices for Spain. Data 2, 22. https://doi.org/10.3390/data2030022.
Vicente–Serrano, S.M., Beguería, S., López–Moreno, J.I., 2010. A multiscalar drought index sensitive to global warming: the standardized precipitation evapotranspiration index. J. Clim. 23, 1696–1718.
Volaire, F., 2018. A unified framework of plant adaptive strategies to drought: crossing scales and disciplines. Glob. Change Biol. 24, 2929–2938.
Warton, D.I., Duursma, R.A., Falster, D.S., Taskinen, S., 2012. smatr 3– an R package for estimation and inference about allometric lines. Methods Ecol. Evol. 3, 257–259. https://doi.org/10.1111/j.2041-210X.2011.00153.x.
Warton, D.I., Wright, I.J., Falster, D.S., Westoby, M., 2006. A review of bivariate line-fitting methods for allometry. Biol. Rev. 81, 259–291.
Wigley, T.M.L., Briffa, K.R., Jones, P.D., 1984. On the average value of correlated time series, with applications in dendroclimatology and hydrometeorology. J. Clim. Appl. Meteorol. 23, 201–213.
Wood, S.N., 2003. Thin plate regression splines. J. R. Stat. Soc. B 65, 95–114.
Wood, S.N., 2017. Generalized Additive Models: An Introduction with R, 2nd edition. Chapman and Hall/CRC.

Yi, K., Dragoni, D., Phillips, R.P., Roman, D.T., Novick, K.A., 2017. Dynamics of stem water uptake among isohydric and anisohydric species experiencing a severe drought. Tree Physiol. 37, 1379–1392. https://doi.org/10.1093/treephys/tpw126.
Zang, C., Biondi, F., 2015. treeclim: an R package for the numerical calibration of proxy-climate relationships. Ecography 38, 431–436.
Zanne, A.E., Westoby, M., Falster, D.S., Ackerly, D.D., Loarie, S.R., et al., 2010. Angiosperm wood structure: global patterns in vessel anatomy and their relation to wood density and potential conductivity. Am. J. Bot. 97, 207–215. https://doi.org/10.3732/ajb.0900178.